Available online at www.sciencedirect.com
ScienceDirect
Cement and Concrete Research 36 (2006) 2123–2131
Cement and Concrete Research

Activation of fly ash cementitious systems in the presence of quicklime. Part II: Nature of hydration products, porosity and microstructure development

S. Antiohos [a,1], A. Papageorgiou [b], S. Tsimas [a,*]

[a] National Technical University of Athens, School of Chemical Engineering, 9 Heroon Polytechniou, Zografou Campus, GR-157 73 Athens, Greece
[b] Independent Researcher, P.O. Box 110, 19 014 Kapandriti, Greece

Received 9 February 2006; accepted 19 September 2006

Abstract

Following the first paper of a two-part series study on the activating effect of industrial quicklime upon different fly ashes, the current paper concludes on its beneficial role by focusing on the nature of hydration products, pore size and microstructure evolution of each system that was investigated. By looking into the development of these properties, the exact effect of the chemical activator could be elucidated, but furthermore a first approximation of the durability efficiency of the examined systems could be obtained. In the frame of this second part, it was demonstrated that, apart from portlandite, calcium sulphoaluminates (ettringite and monosulfoaluminate) along with some gismondine and gehlenite hydrate (C_2ASH_8) crystals are formed in activated fly ash-cement pastes from the first week of hydration. Mercury intrusion porosimetry data confirmed the beneficial action of quicklime, towards decreasing the total pore volume (and concurrent increase in the volume occupied by fine pores) in high-lime ash blends. Gel/space ratios were estimated for each blended paste, and fine, almost linear, correlation was established with total porosity values. Microscopical observations revealed that the critical contribution of quicklime in the production of secondary C–S–H nearby the ash particles. The flocculent-like gel collaborates smoothly with needle-like products and finely-dispersed crystals towards the gradual impletion of the pores and strengthening of the paste.

Keywords: Hydration products (B); Pore size distribution (B); Microstructure (B); Gel/space ratio; Mercury porosimetry (B)

1. Introduction

It has been fairly well demonstrated that not only the strength of concrete, but also its durability, is crucial for extending the service life-time of a structure. The latter factor is of greater importance in cases where secondary cementitious materials are introduced in the mix due to the fact that they have been less tested than Portland cement, but also because of their heterogeneity and different physicochemical properties, factors highly dependant on the nature of the raw feed and processing methods followed [1–4]. For obtaining an idea on the durability efficiency of blended cements, most researchers are performing accelerated tests by exposing specimens to very aggressive simulated environments. However, given that durability properties are highly dependant on the nature of the hydration products formed, as well as with pore size distribution and microstructure development [5–7], the monitoring of such properties is of considerable interest since it can provide a good first indication of the ability of cementitious systems to resist chemical attack.

The majority of scientists dealing with the use of supplementary cementing materials agree that in most cases fly ash improves the properties of concrete. Recently, Chindaprasit et al. [8] tested several concretes containing bulk and processed fly ashes in terms of sulfate resistance and drying shrinkage to find out that both properties were improved with the incorporation of a high ash dosage (i.e. 40% by weight). Excellent concrete performance has also been reported even in projects where fly ash exceeded cement by weight in the total binder

* Corresponding author. Tel.: +30 210 772 3095; fax: +30 210 772 1727.
E-mail addresses: adiochic@central.ntua.gr (S. Antiohos), stangits@central.ntua.gr (S. Tsimas).
[1] Tel.: +30 210 772 2893; fax: +30 210 772 3188.

0008-8846/$ - see front matter © 2006 Elsevier Ltd. All rights reserved.
doi:10.1016/j.cemconres.2006.09.013

volume, as well as in projects where non-standardized fly ashes were utilized [9–11]. Regardless of the methods and specimens used, the investigators seem to conclude that the reaction between the amorphous siliceous body of the ash and hydrated lime (towards the formation of additional pozzolanic C–S–H), is mainly responsible for the beneficial action of the pozzolan.

Normally, the reaction described above is relatively slow, since active silica accumulates in the interior part of the ash sphere, which is very slowly corroded in the cement paste environment [12]. Still, with the aid of several activation techniques, faster reaction rates can be ensured for fly ashes. Bearing that in mind, Saraswathy et al. [13] examined different activation techniques (thermal, chemical and physical) to improve the reactivity of fly ash. All tests performed confirmed that a 20–30% replacement of cement by chemically activated fly ash improved the strength and resistance to corrosion of the final product. Goni et al. [14] treated two kinds of Spanish fly ashes hydrothermally to enhance the pozzolanic reaction. They found out that α-C_2SH, C–S–H gel and a mixed oxide ($CaFe_2O_4$) were formed depending on the kind of the starting material. Puertas et al. [15] performed alkali-activation of fly ash/slag pastes to prove the existence of an alkaline alumino-silicate hydrate with a three-dimensional structure as a result of fly ash activation. SEM examination confirmed that the reaction that produced the above hydrate occurred around fly ash particles. Earlier, Katz [16] had used electron microscopy to explain the activation effect of alkaline solutions, such as NaOH, at different concentrations, temperatures, and water-to-fly ash ratios. The results obtained provided strong evidence that fly ash activation depends not only on the pH of the activating solution but on the ratio between the solution and the fly ash as well.

In this second part of this study, the hydration, porosity, gel/space ratios and microstructural development of blended cements prepared with quicklime-activated fly ashes were examined. The principal goal of this investigation was to affirm the activating effect of quicklime discussed in the first part of this study [17]. Furthermore, by looking into the nature of the generated products and microstructure developed with age in each case (different types of fly ashes and additions of quicklime were used) the authors aimed to obtain an initial impression of the potential durability of the examined systems.

2. Experimental section

2.1. Materials

Details regarding the starting materials (cement, fly ashes and chemical activator) and the construction of the paste samples are given in the first part of the study [17]. It is reminded that two class C ashes (T_f and T_d) and one class F ash (T_m) were used. T_f has a high content of active silica and rather moderate percentage of reactive CaO, whilst T_d has a normal active silica content (around 25% by weight) and an unusually high amount of active lime (reaching 26%). With regard to their other principal chemical properties, the two class C ashes possess similar amounts of alumina, sulfur trioxide and free lime. T_m is a typical low-calcium fly ash with high active silica and almost no free lime. After being ground to reach similar finenesses (5450, 5600 and 5550 cm^2/g Blaine values were measured for T_f, T_d and T_m, respectively), industrial quicklime was added (as the chemical activator), replacing an equal mass of fly ash in each mix. In the case of high-calcium ashes, a 3 and 6% fly ash replacement was adopted, whilst in the case of T_m ash, higher replacements (i.e. 5, 10 and 15% by weight of fly ash) were applied to compensate for its low lime content. The new blends were named after the ash incorporated and the amount of quicklime added. For example,

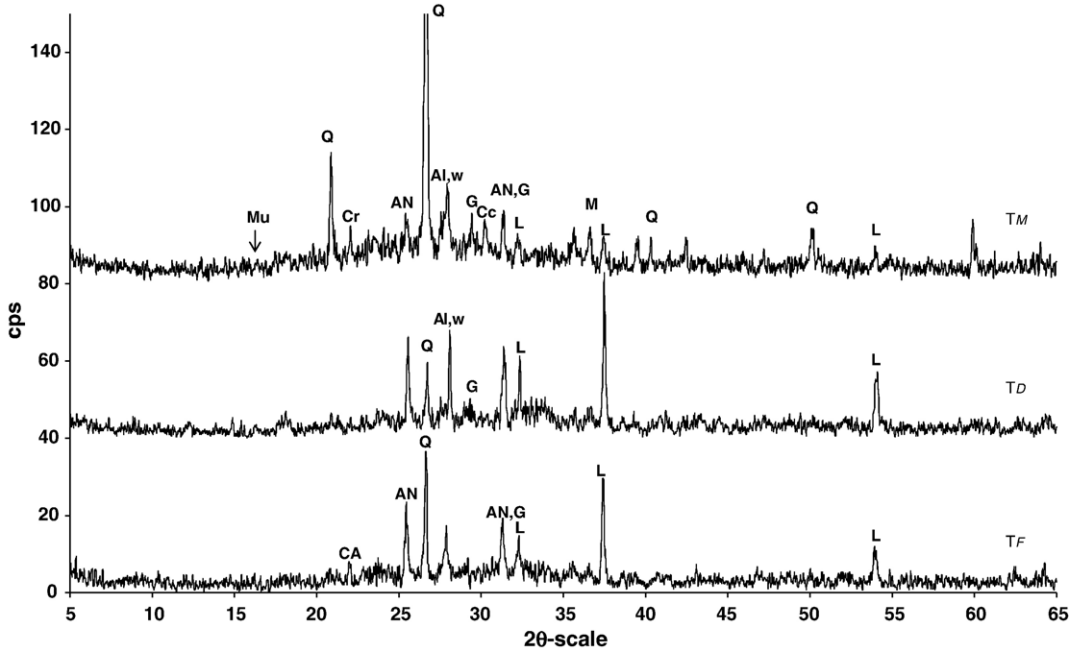

Fig. 1. X-Ray diffraction spectra of utilized fly ashes (Q: Quartz, L: Lime, Cr: Cristobalite, AN: Anhydrite, Mu: Mullite, M: Magnetite, w: Wollastonite, CA: C_3A, Cc: Calcite, Al: Albite).

T_f–6c corresponds to the specimen prepared when quicklime replaced 6% by weight T_f ash. Paste samples were prepared with water: binder ratio (w/b) of 0.5, with the binder substituting 20% by weight of cement in all specimens. Keeping the w/b ratio constant, a cement paste without any fly ash or quicklime was prepared as the control specimen.

The physicochemical characterization of the raw ashes was completed with the identification of their crystalline compounds. This was achieved with the use of a Siemens D 5000 X-ray diffractometer (CuK_a radiation, 40 KV, 30 mA) in a scanning range of 5 to 65° in 2θ scale. The testing rate applied was 0.02°/s for all specimens and identification of the products was carried out by using a Diffrac-At Database. The predominant crystalline constituents of the fly ashes are presented in Fig. 1, where their XRD spectra are plotted. Peaks indicating the presence of quartz, anhydrite, gypsum and lime are evident in all samples, with quartz being more intense in the case of silica rich T_m and T_f ashes and lime in both high calcium ashes. Traces of albite and wollastonite are also present, as well as mullite. Mullite and cristoballite contain primarily silicon dioxide and are only detectable in the case of low-calcium ash. No significant difference was detected among the XRD spectra of the raw and ground ashes, indicating that mechanical grinding had no effect on the nature of the crystalline constituents of all samples tested.

2.2. Testing methods

For detecting possible alterations in the nature of hydration products, selected paste samples (in powder form) were tested with the use of X-Ray Diffraction (XRD) after one and twelve weeks of hydration. Testing parameters are given in Section 2.1. The samples for the Mercury Intrusion Porosimetry (MIP) were obtained from the core of the fractured pastes, after being soaked in organic solvents, at selected curing times. The analytical procedure followed for terminating hydration is also described in the first part of this work. Porosity measurements were performed in a 'Porosimeter 2000' (Fisons Instruments) mercury intrusion porosimeter with a maximum mercury intrusion pressure of 2000 bar. Cylindrical pore geometry and a contact angle θ of 141.3° were assumed. The mercury intruded pore diameter d_p at an intrusion pressure of P_{In} was calculated by $d_p = -4\gamma\cos\theta/P_{In}$, where γ the surface tension of mercury (equal with 0.480 Nm^{-1}).

Finally, a XL 30 Philips Scanning Electron Microscope equipped with an Energy Dispersive X-Ray Analyzer (EDX) was used to obtain a view of the microstructure of the activated systems and to conduct an elemental analysis of the accumulated hydration products. Semi-quantitative analysis was performed on polished surfaces of representative fragments of pastes.

3. Results and discussion

3.1. Identification of hydration products

Examination of the pastes with XRD assisted observations based on thermal analysis data, formulated in part I, which revealed the strong presence of calcium hydroxide and ettringite in almost all activated samples. Significant presence of portlandite, throughout the curing period, is also confirmed in the XRD patterns of the T_d and T_f fly ash pastes as shown in Figs. 2 and 3 respectively. In fact, this is the principal crystalline

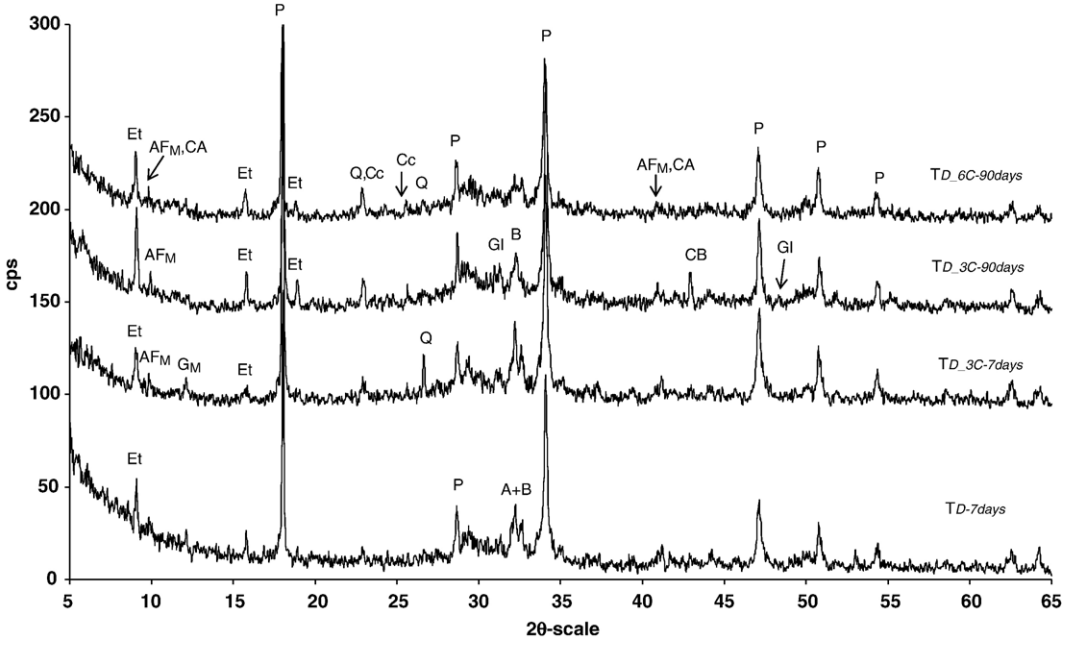

Fig. 2. XRD spectra of initial and quicklime-activated T_d fly ash pastes with curing age (Et: Ettringite, CA: Calcium aluminum oxide hydrate, G_M: Gismondine, P: Portlandite, Cc: Calcite Q: Quartz, A: Alite, B: Belite, AF_M: Calcium aluminum sulfate hydrate, Gl: Gehlenite hydrate, CB: Calcium Aluminum Oxide Carbonate Hydrate).

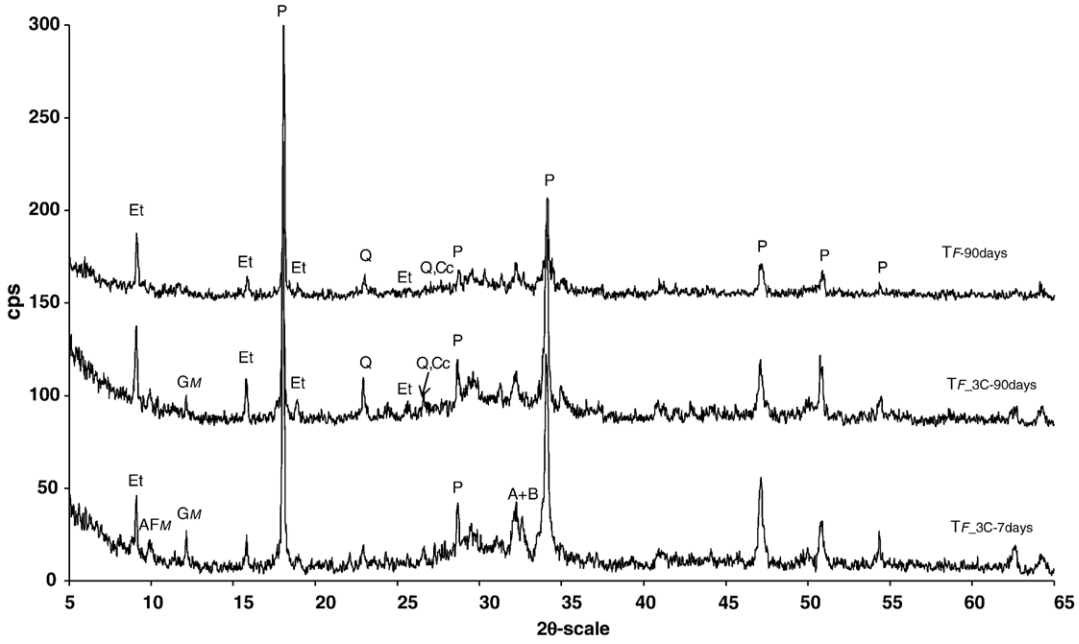

Fig. 3. XRD spectra of initial and quicklime-activated T_f fly ash pastes with curing age (Et: Ettringite, G_M:Gismondine, P: Portlandite, Cc: Calcite Q: Quartz, A: Alite, B: Belite, AF_M: Calcium aluminum sulfate hydrate, Gl: Gehlenite hydrate).

product along with ettringite ($Ca_2Al_2(SO_4)_3{\cdot}32H_2O$) and monosulfoaluminate phases ($Ca_4Al(SO_4){\cdot}18H_2O$) which form as early as 7 days of hydration and persist until the end of the testing period. It is known that, when controlled, the continuing formation of ettringite can result in excellent hydraulic performance [18]. The formation of ettringite can contribute to early strength development [18,19], and in the case investigated here, it is possible that it assists strength development at later ages from the formation of C–S–H (the major phase present in the paste). Small addition of quicklime (T_d_3C) and subsequent acceleration of pozzolanic reaction (as shown in part I) led to the early formation of gismondine and some gehlenite hydrate. These compounds are able to fill the pores of the paste making a contribution to the superior strength

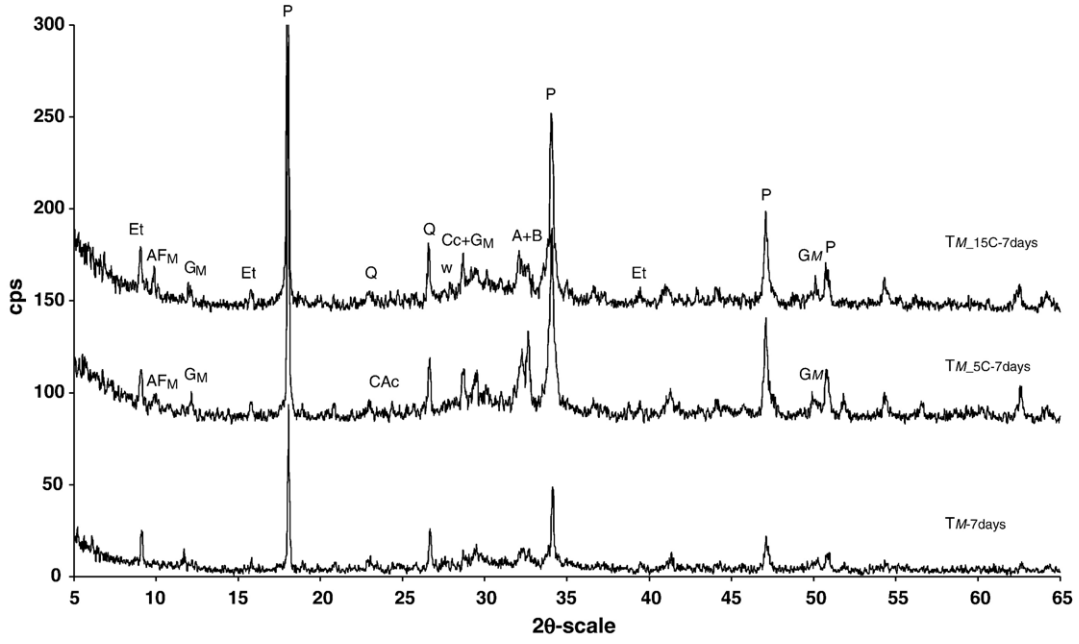

Fig. 4. XRD spectra of initial and quicklime-activated T_m fly ash pastes with curing age (Et: Ettringite, G_M: Gismondine, P: Portlandite, Cc: Calcite Q: Quartz, A: Alite, B: Belite, AF_M: Calcium aluminum sulfate hydrate, W: Wollastonite, CAc: $C_4ACO_3H_{11}$).

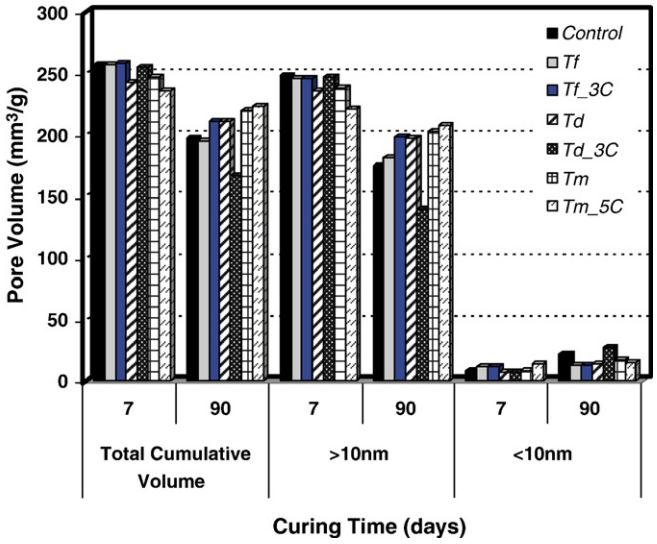

Fig. 5. Pore size distribution in quicklime-activated fly ash blended cements.

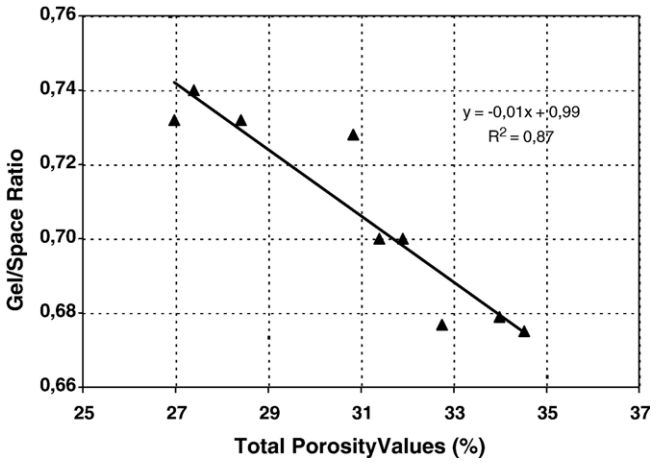

Fig. 6. Correlation of gel/space ratios and porosity values at the end of curing.

of the activated system. The absence of any alite peaks after 90 days (contrary to what is observed in the case of T_d and T_d–6C pastes) in the same blend could indicate that such an addition of CaO (along with dilution effect [12,20]) enhanced the hydration of the clinker's main constituent.

Similar crystalline products are detected in the case of the second high-lime fly ash series (T_f). In that case the presence of gismondine in the activated paste is more intense after the first week of curing. Since gismondine ($CaAl_2Si_2O_8{\cdot}4H_2O$) is a hydrated compound that contains silicon dioxide, it is believed that this is the outcome of the accelerating action of quicklime that initiated the faster dissolution of amorphous silica from high siliceous active T_f ash particles and its incorporation into the gismondine structure. With regard to the quicklime addition in low-lime T_m ash pastes, it can be noticed (Fig. 4) that monosulfoaluminate forms very soon, presumably from ettringite transformation [18,21]. Peaks corresponding to the presence of ettringite are detectable here as well but not so intense compared to the respective peaks in the systems with high-lime ashes. That implies that less ettringite is formed in blends with lower-lime fly ash as a result of the negligible presence of anhydrite in the raw ash (see Fig. 1). This observation is consistent with the work of Tishmack et al. [22], who noted that ettringite formation increases with increasing anhydrite levels. Results confirm previous remarks regarding the continuous presence of portlandite throughout the testing period. This becomes even clearer in the pattern of T_m–15C paste where hydrated quicklime remained inactive in the matrix. It is therefore possible that the carbonate hydrates detected in both samples after 90 days are caused by the carbonation of unbound calcium hydroxide.

Table 1
Gel/space ratios of initial and quicklime-activated FC pastes with curing time

Specimen	Gel/space ratios			
	2	7	28	90
Control	0.462	0.478	0.606	0.645
T_f	0.413	0.524	0.594	0.700
T_f–3c	0.464	0.525	0.640	0.700
T_f–6c	0.470	0.518	0.603	0.727
T_d	0.438	0.526	0.573	0.677
T_d–3c	0.480	0.521	0.624	0.732
T_d–6c	0.483	0.511	0.645	0.738
T_m	0.435	0.577	0.650	0.679
T_m–5c	0.421	0.560	0.657	0.675
T_m–15c	0.413	0.559	0.648	0.732

3.2. Pore size distribution

During the MIP examination, apart from determining the total pore volume, the authors aimed at monitoring the variation of the gel pores (i.e. pore diameter <10 nm) with age. This is due to the distinction existing between the capillary and gel pores created in a hydrated cement paste and the fact that the latter are regarded as an intrinsic part of C–S–H (strength providing gel) whilst the former are considered as remnants of water-filled space [23]. Results plotted in Fig. 5 demonstrate that the percentage of the total pore volume decreases with quicklime addition and curing time for the blends containing high calcium ashes. This is probably the outcome of the continuous generation of pozzolanic reaction products that fill the pores. Data shown in the same figure reveal that the percentage of the fine pore volume (FPV) increases with continuous hydration and activator percentage. With respect to FPV, an important increase is observed in the case of T_d–3C, at the end of the curing period, a fact that coincides with the excellent strength performance of the same blend as pointed out in part I of this study. On the contrary, the limited activating effect of quicklime on the reaction rate of low-calcium ash is confirmed from the temporal decrease of the total pore volume of the T_m–5C paste (in relation to T_m) after the first week of hydration and the consecutive increase of the same factor at 90 days. The fact that during the two presented curing stages, the FPV percentage of the same blend stays practically the

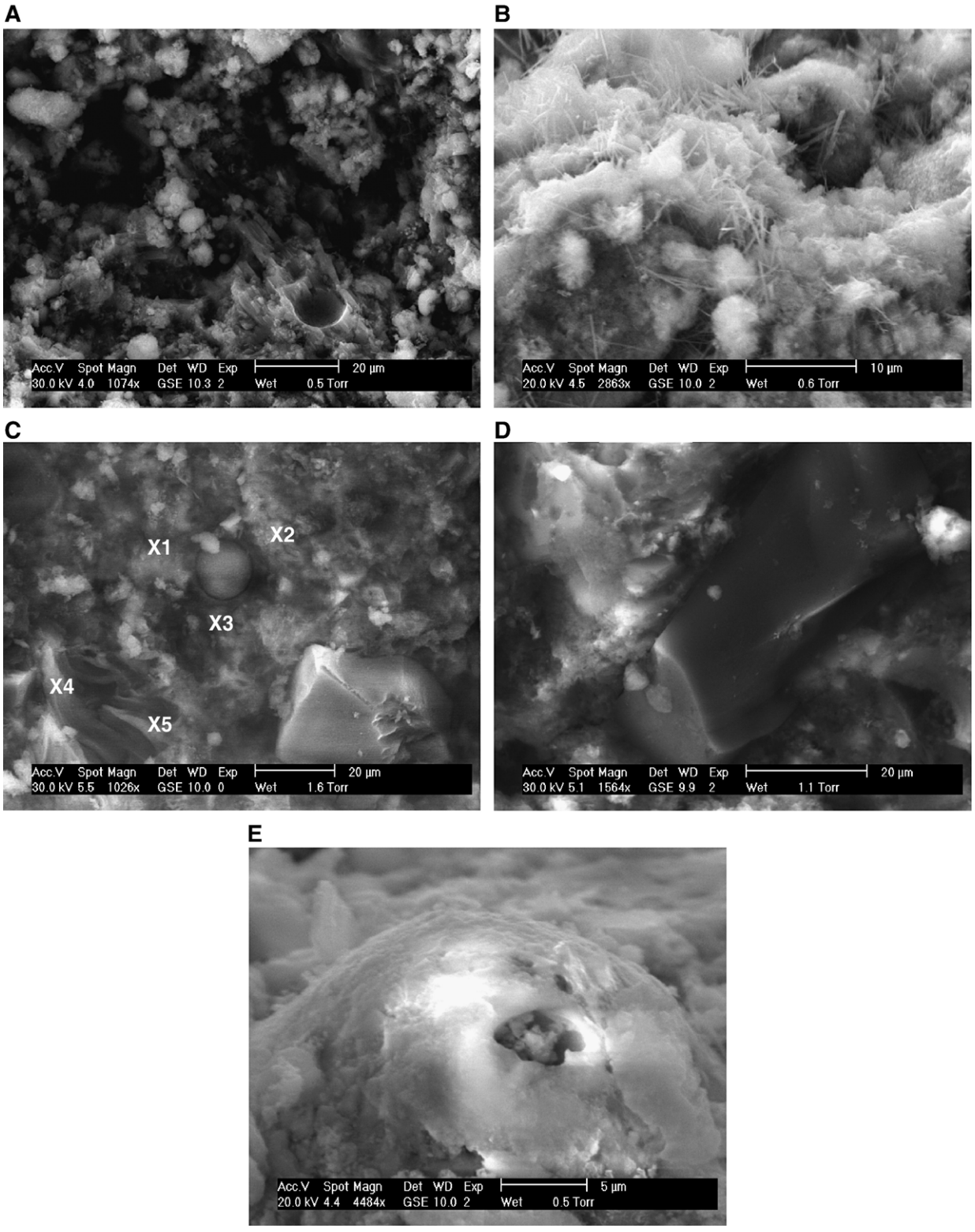

Fig. 7. (A). Unreacted fly ash particles and visible voids in the matrix of T_d paste after the first week of curing. (B). Ettringite accumulation in T_d–3C paste after 7 days of curing. (C). Massive C–S–H production around ash particle in the matrix of T_d–3C paste (90 days of curing). (D). Crystal of gismondine (center of the photo) intercepting C–S–H and CH generation. (E). SEM photo of T_m particle encircled by CH after 90 days in 15% lime-activated T_m paste.

same (14.52 mm^3/g at 7 days and 15.31 mm^3/g at 90 days respectively), confirms the absence of any activating action by quicklime included in the mix. Lin et al. [24], have recently postulated that another reason for the pore size variation that may occur in pozzolanic pastes could be the production of swelling (and subsequent decrease of the fine pore volume) due

to the formation of several calcium sulfate hydrates, such as ettringite and monosulfoaluminate. The validity of this argument in the content of the present work is debatable since XRD evidence denoted that the presence of the aforementioned compounds (in low-calcium ash specimens) reduces with hydration age.

3.3. Gel/space ratios and correlation with mercury intrusion porosity

Gel/space ratio is defined as the ratio of the volume occupied by hydrated cement to the sum of the volumes occupied by hydrated cement and by capillary pores that are present in the matrix. According to Neville [25], cement hydrates occupy more than twice their original volume; thus the products of hydration of 1 ml of cement will be assumed to occupy 2.06 ml and the gel/space ratio (X_c) can be calculated according to the following equation:

$$X_c = \frac{2.06 v_c a_c}{v_c a_c + \frac{w}{c}} \quad (1)$$

where, v_c is the specific volume of anhydrous cement, α is the degree of cement hydration at a given curing stage, and w/c is the water-to-cement ratio used for preparing the paste.

The application of the above equation in the case of concrete and paste prepared with blended cements is debatable as implied by the conflicting works published on the issue. Especially with regard to the use of fly ash and given that exact volume stoichiometry of the pozzolanic reactions has not been established, the formulation seems to be even less certain. Lam et al. [26] for example, worked in this direction by trying to incorporate the stoichiometry of the pozzolanic reaction (based on a model developed earlier by Bentz and Garboczi [27]) into Eq. (1). They arrived at a modified scheme that takes into consideration the density, reaction degree of fly ash and the effective w/c ratio. Such a modification of the initial expression for the gel/space ratio was however, imperative since the authors worked with high volumes of fly ash pastes, a fact that obviously causes significant changes in the hydration evolution of the final product [9,20]. On the other hand, Heikal [28] applied the equation described above unaltered to determine the gel/space ratios of pozzolanic specimens as well. In the present work, because of the low level cement replacement (i.e. 20% by weight), the similarities observed in the nature of the hydration products and the fact that the dosage of the chemical activator added is not only negligible but of the same chemical constituents contained in the raw materials (cement and fly ashes), the authors postulated that hydration degrees of the examined systems could be derived from data of chemical combined water presented in the first part of the study.

Based on the above assumption, the measured density of cement (3.19 corresponding to a value of $v_c = 1/3.19 = 0{,}313$) and the W/C 0,5 ratio applied in all pastes, a detailed description of the gel/space ratio calculation is provided below, as an example for the case of T_f–3C paste after one month of hydration. According to data presented in part I of the study, the non-evaporable water (W_n) content of the specific sample after 28 days of hydration was found to be 16.57%, whilst a fully hydrated cement paste is assumed to have a W_n content of approximately 23% [12,20]. Therefore, in this case, $_{ac} = 16.57/23 = 0.72$ and subsequently when inserted in Eq. (1) the gel/space ratio X_c is 0.624. The calculated results shown in Table 1 indicate that in the case of high-calcium fly ash pastes, the incorporation of quicklime results in a relatively important increase in the gel/space ratios from the beginning of hydration. This is due to the accelerating effect of quicklime on the fly ashes pozzolanic action, which leads to the formation of additional C–S–H gel. The latter obviously accounts for the subsequent increase of the volume occupied by hydrated compounds. Contrarywise, the negligible activating effect that quicklime addition had on the blends utilizing low-lime ash is highlighted through the concept of the gel/space ratio. This becomes clear from the decrease of their gel/space ratios with quicklime addition during the testing period.

When plotting the total porosity data against the data derived for the gel/space ratio for fly ash-cement and quicklime-activated fly ash-cement pastes (Fig. 6), after three months of hydration, it can be observed that they correlate almost linearly. The close agreement of the experimental data (MIP measurements) with the data derived from the use of a theoretical expression for gel/space ratio, confirms the validity of the assumptions stated previously and furthermore the close relationship between the gel/space ratio development and the gradual infilling of the pores existing in the matrices.

3.4. ESEM observations

During the SEM examination special attention was paid to the fly ash-cement pastes where quicklime addition had the greatest impact (T_d ash pastes). Pastes with low-calcium fly ash (in which quicklime had no activating effect) were also monitored for comparison purposes. Fig. 7(A) is a typical image of the microstructure of the T_d paste, before quicklime addition, after the first week of hydration. Unreacted fly ash particles retaining their smooth and spherical shape are easily distinguishable, while some others have already been covered by calcium hydroxide (product of hydration). It is well known that at such an early age, the majority of fly ash particles do not react (under normal hydrating conditions), and they act as additional nucleation centers for promoting the precipitation of hydrated compounds [12,29]. Numerous voids visible indicate the presence of large pores in the matrix as commented in

Table 2
Ca/Si ratios of C–S–H gels formed in different areas of the T_d–3C matrix after 90 days of curing (as these are depicted in Fig. 7(C))

	Position of analysis	Ca/Si ratio	CSH characterization
X1	Nearby the ash particle	1.43	Pozzolanic
X2	Nearby the ash particle	1.38	Pozzolanic
X3	Nearby the ash particle	1.56	Pozzolanic
X4	Away from ash particle	1.82	Cementitious
X5	Away from ash particle	2.11	Cementitious

Section 3.2. Upon 3% quicklime addition (Fig. 7(B)), it can be noticed that fiber-shaped C–S–H extends from fly ash particles while rodlets of AF_t phases (produced from the reaction of lime and rich-in-SO_3 fly ash) are also dominant in the paste. Studies conducted from the sixties [30] have shown that ettringite (and monosulfate hydrates as well) may be formed easily in fly ash mixtures with lime.

Voids visible after the first week decrease substantially with curing time as a result of the continuous accumulation of more hydration products (as indicated by increasing non-evaporable water values). In Fig. 7(C), the SEM photo of the T_d–3C paste after three months of curing is shown. At this age, flocculent C–S–H gel surrounds the majority of the particles. EDX analyses on the surrounding area, confirmed the presence of silica rich C–S–H, denoting the progress of the pozzolanic reaction. The latter observation is confirmed by data summarized in Table 2, where the Ca/Si ratio of C–S–H gels after 90 days of curing in the same sample, formed in different areas in the matrix, were determined with the aid of EDX analysis. The binding properties of this gel supplement the filling effect of the ashes that remain intact, leading to a subsequent decrease of the pores in the paste. In other parts of the same paste (Fig. 7 (D)), large crystals were identified. Microanalysis revealed the presence of gismondine, which coincides with data derived during XRD examination. Such crystals were found to be dispersed in the paste, intercepting massive C–S–H gel. In most cases they are finely incorporated between the main hydration products, decreasing the pores, thus hardening the paste.

In general, in the pastes incorporating lower-lime fly ash, hydration products observed were less complex than those detected in high-lime paste. This could be due to the presence of reactive crystalline compounds contained in high-lime ashes (such as anhydrite and lime) and more active calcium aluminosilicate glass phase. In this case, a small quicklime addition (T_m–5C) did not alter the microstructure of the initial binary blend. Despite accelerated fly ash reaction during the first week, SEM examination revealed that many ash particles remained intact even after 28 days of hydration. The fact that even at the end of the curing period, fly ash particles were found to be extensively surrounded by CH (Fig. 7(E)), provides an additional indication that the excess of portlandite caused by quicklime introduction, acted inhibitory for the action of fly ash. The latter observation is in accordance with remarks formulated by Grutzeck [31] who noticed that extensive surrounding of fly ash particles by calcium hydroxide resulted in a substantial limitation of the reactivity of the particles. That possibly accounts for the negative effect of added quicklime on the action rate of low-lime ash discussed on the first part of this work.

4. Conlcusions

Improving the performance of fly ash blended cements is of great importance for numerous stakeholders of the construction sector. In this second part of a two-part study, certain key factors governing the performance of quicklime-activated fly ash-cements were identified. Due to the lack of relevant data in the literature, the authors attempted to elucidate the nature and morphology of generated hydration products, pore size distribution and gel/space ratios, as well as microstructural development of activated ash pastes. From the investigation of the above the following main conclusions may be drawn:

(1) Portlandite and calcium sulphoaluminates (mainly ettringite and monosulfoaluminate) were the main hydration products formed in the activated fly ash pastes. The presence of the latter compounds was greater in the case of high-lime ashes, as a result of the reaction between hydrated lime and the SO_3 they contain. Gismondine and some gehlenite hydrate were also detected in quicklime-activated pastes after the first week of hydration. It is believed that the generation of these products is favored by the faster liberation of amorphous silica from the glass of the ashes in the presence of the activator. Such compounds are considered partly responsible for the compaction of the paste and thus reduction of the system's porosity.

(2) Small addition of quicklime decreased the total pore volume of activated high-lime ash pastes and simultaneously increased notably the volume occupied by fine pores. On the contrary, despite the presence of quicklime, the total porosity of low-calcium ash pastes was only slightly reduced after the first week and increased thereafter. This confirmed the absence of any later age activating effect of quicklime.

(3) Gel/space ratios were determined on the basis that the degree of cement hydration which could be estimated with the use of non-evaporable water values. This was regarded as a feasible approach given the low level cement replacement, the absence of any considerable disparities in the nature of the generated products and the small amount of activator supplied in the pastes. It was shown that the incorporation of quicklime into fly ash-cement pastes resulted in a notable increase of the gel/space ratios from the beginning of hydration. This was due to the accelerating effect of quicklime on the rate of pozzolanic reaction, which favored the accumulation of additional C–S–H gel. An almost linear correlation established between the total porosity data and the gel/space ratios confirmed the validity of the expression used.

(4) Microscopy examination confirmed the presence of the main crystalline hydration products (already identified with the aid of X-Ray Diffraction) and the continuous generation of amorphous pozzolanic C–S–H in the surrounding area of the ash particles. Microanalysis affirmed the presence of gismondine, whose crystals were found to be either dispersed in the paste (intercepting massive C–S–H gel), or finely incorporated between the main hydration products. Many low-lime ash particles were found to be extensively surrounded by CH, even after one month of curing. This provided an additional indication that the excess of portlandite created by quicklime introduction, acted as an inhibitor for the reaction of low-lime fly ash.

Aknowledgements

The assistance of Mrs. S. Anagnostopoulou during the MIP investigation is highly appreciated. Grateful acknowledgement is extended also to Mr. A. Bakolas for his insightful remarks during the evaluation of porosimetry results. **[M.B.]**

References

[1] Stanislav V. Vassilev, Rosa Menendez, Diego Alvarez, Mercedes Diaz-Somoano, M. Rosa Martinez-Tarazona, Phase-mineral and chemical composition of coal fly ashes as a basis for their multicomponent utilization. 1. Characterization of feed coals and fly ashes, Fuel 82 (14) (2003) 1793–1811.

[2] Vassiliki Sakorafa, Kleopas Michailidis, Francesco Burragato, Mineralogy, geochemistry and physical properties of fly ash from the Megalopolis lignite fields, Peloponnese, Southern Greece, Fuel 75 (4) (1996) 419–423.

[3] T. Mangialardi, Disposal of MSWI fly ash through a combined washing-immobilisation process, J. Hazard. Mater. 98 (1–3) (2003) 225–240.

[4] L.K. Sear, UK practice — a review of fly ashes for use in concrete, PROGRES Workshop on Novel Products from Combustion Residues, Morella, Spain, 2001.

[5] A.A. Ramezanianpour, M. Malhotra, Effect of curing on the compressive strength, resistance to chloride-ion penetration and porosity of concretes incorporating slag, fly ash or silica fume, Cem. Concr. Compos. 17 (2) (1995) 125–133.

[6] M.H. Zhang, Microstructure, crack propagation, and mechanical properties of cement pastes containing high volumes of fly ashes, Cem. Concr. Res. 25 (6) (1995) 1165–1178.

[7] S. Antiohos, S. Tsimas, Chloride resistance of concrete incorporating two types of fly ashes and their intermixtures, The Effect of Active Silica Content, Proceedings of the 6th International Conference on Durability of Concrete, Thessaloniki, 2003, p. 115, Supplementary Papers.

[8] P. Chindaprasirt, S. Homwuttiwong, V. Sirivivatnanon, Influence of fly ash fineness on strength, drying shrinkage and sulfate resistance of blended cement mortar, Cem. Concr. Res. 34 (7) (2004) 1087–1092.

[9] N. Bouzoubaâ, M.H. Zhang, M. Malhotra, Mechanical properties and durability of concrete made with high-volume fly ash blended cements using a coarse fly ash, Cem. Concr. Res. 31 (10) (2001) 1393–1402.

[10] Linhua Jiang, Zhenqing Liu, Yiqun Ye, Durability of concrete incorporating large volumes of low-quality fly ash, Cem. Concr. Res. 34 (8) (2004) 1467–1469.

[11] C.S. Poon, X.C. Qiao, Z.S. Lin, Pozzolanic properties of reject fly ash in blended cement pastes, Cem. Concr. Res. 31 (11) (2003) 1857–1865.

[12] S.N. Ghosh, L.S. Sarkar, Mineral admixtures in cement and concrete, Progress in Cement and Concrete, 1st ed., ABI Books, New Delhi, 1993, p. 565.

[13] V. Saraswathy, S. Muralidharan, K. Thangavel, S. Srinivasan, Influence of activated fly ash on corrosion-resistance and strength of concrete, Cem. Concr. Compos. 25 (7) (2003) 673–680.

[14] S. Goñi, A. Guerrero, M.P. Luxán, A. Macías, Activation of the fly ash pozzolanic reaction by hydrothermal conditions, Cem. Concr. Res. 33 (9) (2003) 1399–1405.

[15] F. Puertas, A. Fernández-Jiménez, Mineralogical and microstructural characterisation of alkali-activated fly ash/slag pastes, Cem. Concr. Compos. 25 (3) (2003) 287–292.

[16] A. Katz, Microscopic study of alkali-activated fly ash, Cem. Concr. Res. 28 (2) (1998) 197–208.

[17] S. Antiohos, S. Tsimas, Activation of fly ash cementitious systems in the presence of quicklime. Part I. Compressive strength and pozzolanic reaction rate, Cem. Concr. Res. 34 (5) (2004) 769–779.

[18] Lawrence D. Adams, Ettringite, the positive side, Proceedings of the 19th International Conference on Cement Microscopy, Cincinnati, Ohio, April 27–May 1, 1997, pp. 1–13.

[19] G. Verbeck, Cement Hydration Reactions at Early Ages, Research and Development Information, PCA R&D Serial No. 189, Portland Cement Association, 1965.

[20] E.E. Berry, R.T. Hemmings, B.J. Cornelius, Mechanisms of hydration reactions in high volume fly ash pastes and mortars, Cem. Concr. Compos. 12 (4) (1990) 253–261.

[21] J. Havlica, S. Sahu, Mechanism of ettringite and monosulphate formation, Cem. Concr. Res. 22 (4) (1992) 671–677.

[22] J.K. Tishmack, J. Olek, S. Diamond, Characterization of high-calcium fly ashes and their potential influence on ettringite formation in cementitious systems, Cem. Concr. Aggreg. 21 (1) (1999) 82–92.

[23] S. Mindess, J.F. Young, D. Darwin, Concrete, Second ed., Prentice-Hall, NJ, 2003.

[24] K.L. Lin, K.S. Wang, B.Y. Tzeng, N.F. Wang, C.Y. Lin, Effects of Al_2O_3 on the hydration activity of municipal solid waste incinerator fly ash slag, Cem. Concr. Res. 34 (4) (2004) 587–592.

[25] A.M. Neville, Properties of Concrete, Fourth and Final ed., Longman, 1995.

[26] L. Lam, Y.L. Wong, C.S. Poon, Degree of hydration and gel/space ratio of high-volume fly ash/cement systems, Cem. Concr. Res. 30 (5) (2000) 747–756.

[27] D.P. Bentz, E.J. Garboczi, Simulation studies of the effects on mineral admixtures on the cement paste-aggregate interfacial zone, ACI Mater. J. 88 (5) (1991) 518–529.

[28] Mohamed Heikal, Effect of calcium formate as an accelerator on the physicochemical and mechanical properties of pozzolanic cement pastes, Cem. Concr. Res. 34 (6) (2004) 1051–1056.

[29] Nemat Tenoutasse, Anne-Marie Marion, Mechanism of hydration of cement blended with fly ashes, Proceedings of Blended Cements symposium, ASTM Special Technical Publication, Geoffrey Frohnsdorff, Denver, 1984, pp. 65–85.

[30] L.J. Minnick, Proceedings of the Edison Electric Industry, Natural Coal Association and Bureau of Mines Symposium, Fly Ash Utilization, 1967, US.

[31] M.W. Grutzeck, D.M. Roy, B.E. Scheetz, Hydration mechanisms of high-lime fly ash in Portland-cement composites, Proceedings of the Materials Research Symposium, MRS-N, 1981, pp. 92–101.